On the Structure of Molten and Amorphous $Cu_{84.3}P_{15.7}$ by X-ray Diffraction

R. M. Hagenmayer, P. Lamparter, and S. Steeb

Max-Planck-Institut für Metallforschung, Institut für Werkstoffwissenschaft, Seestraße 92,
D-70174 Stuttgart

Z. Naturforsch. **50a,** 931–934 (1995); received July 25, 1995

The atomic distances in molten $Cu_{84.3}P_{15.7}$ at 770 °C are smaller than those in the amorphous state at room temperature. This follows from the pair correlation functions obtained from the total structure factors. Since the weighting factors are rather inconvenient, it is not possible to draw conclusions concerning short range order in amorphous or molten $Cu_{84.3}P_{15.7}$.

Small angle scattering with the amorphous specimen shows up regions with a radius of gyration of 14 Å, whose density is different from the surrounding matrix.

1. Introduction

Amorphous $Co_{80}P_{20}$ and $Ni_{81}P_{19}$ can be easily produced by different methods such as melt spinning [1, 2], sputtering [2] or electro-deposition [2]. Amorphous $Cu_{84.3}P_{15.7}$ could not be produced by splat cooling [3] but could be produced by sputtering. Solid amorphous alloys show usually a splitted second peak in the structure factor. In [1, 4, 5] it was shown that those melts, which can be rapidly cooled to yield amorphous alloys, show at least a shoulder in the second peak of the structure factor.

In the present work, X-ray diffraction was done with molten and amorphous $Cu_{84.3}P_{15.7}$ [6].

2. Theoretical and experimental fundamentals

Concerning the theoretical and experimental fundamentals of X-ray diffraction with molten and amorphous alloys we refer to [6].

The eutectic $Cu_{84.3}P_{15.7}$ alloy with its melting point at 714 °C was produced in a graphite crucible by induction heating of Cu_3P (99.5%) and copper (99.9%). The obtained material was first used for the θ-θ-EDXD investigation of the molten alloy and then as starting material for the production of a sputter target. The sputter parameters were $7 \cdot 10^{-6}$ mbar vacuum; $8 \cdot 10^{-3}$ mbar Argon pressure; 0.06 A cathode current; 0.6 kV high voltage; 0.5 kV DC-potential; and 48 h sputter time. The substrate during sputtering was Al-foil. The Al-foil was removed from the sputtered material by NaOH.

The measured density of the amorphous material was corrected with the thermal expansion coefficient of solid Cu to obtain the density of molten $Cu_{84.3}P_{15.7}$ at 770 °C, which amounts to 6.77 g/cm^3, corresponding to a mean atomic density $\varrho_0 = 0.07$ atoms/Å^3.

X-ray diffraction of the molten alloy was done with the EDXD method [6], and of the amorphous alloy with fast diffractometry, i.e. using a θ-2θ diffractometer (Siemens type D500) in transmission and using a position sensitive detector which detects the angle region $\Delta 2\theta = 15°$ simultaneously [7].

3. Results and Discussion

3.1 Molten $Cu_{84.3}P_{15.7}$

Figure 1 shows in the lower part the Faber-Ziman structure factor as obtained by the EDXD-method from molten $Cu_{84.3}P_{15.7}$. The main maximum lies at $Q = 3.12$ Å^{-1} (height 2.19; full width at half maximum height = FWHM = 0.56 Å^{-1}) and is symmetric, as is the second maximum at 5.60 Å^{-1} (width 1.39 Å^{-1}). The position of the third maximum lies at 8.13 Å^{-1} (width 1.43 Å^{-1}). As will be shown later, the peak at $Q = 1.45$ Å^{-1} (height 0.47; width 0.52 Å^{-1}) is not a prepeak, i.e. it is not determined by the Bhatia Thornton concentration-concentration structure factor $S_{CC}(Q)$ and therefore is called secondary peak. All data from the structure factor are compiled in Table 1. Figure 2 shows as solid line the total pair correlation function as obtained from Fig. 1, lower curve.

Reprint requests to Prof. S. Steeb.

0932-0784 / 95 / 1000-0931 $ 06.00 © – Verlag der Zeitschrift für Naturforschung, D-72027 Tübingen

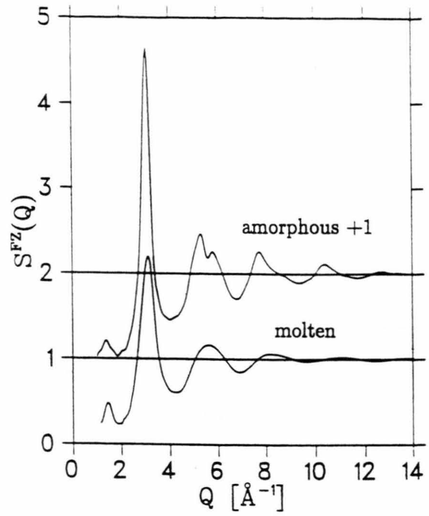

Fig. 1. Total structure factors from $Cu_{84.3}P_{15.7}$; X-rays; A morphous state; ADXD (Mo-K_α).
Molten state (760 °C); EDXD-method.

Table 1. Molten $Cu_{84.3}P_{15.7}$ at 760 °C and amorphous $Cu_{84.3}P_{15.7}$ at room temperature. Structure factor. Peak position, peak height, and full width at half maximum (FWHM).

		$Cu_{84.3}P_{15.7}$ melt	$Cu_{84.3}P_{15.7}$ amorphous
Secondary peak	position [Å^{-1}]	1.45	1.36
	height	0.47	0.21
	FWHM [Å^{-1}]	0.52	0.65
First peak	position [Å^{-1}]	3.12	3.07
	height	2.19	3.63
	FWHM [Å^{-1}]	0.56	0.42
Second peak	position [Å^{-1}]	5.60	5.29
	height	1.16	1.47
	position [Å^{-1}]	–	5.79
	height	–	1.26
	FWHM [Å^{-1}]	1.39	1.27
Third peak	position [Å^{-1}]	8.13	7.74
	height	1.06	1.26
	FWHM [Å^{-1}]	1.43	0.84

The average distance of nearest neighbours amounts to 2.46 Å (FWHM = 0.46 Å) and the number of nearest neighbours amounts to $Z_1 = 12.1$ atoms. Whereas the first peak is symmetric, one observes an asymmetry of the second peak which lies at 4.37 Å and shows a shoulder at 4.77 Å. The average distance of the complete second peak from the origin amounts to 4.56 Å (FWHM = 0.94 Å; $Z_2 = 49.2$ atoms). The third coordination sphere lies at 6.48 Å (FWHM = 0.94 Å).

3.2 Amorphous $Cu_{84.3}P_{15.7}$ and comparison with the melt

As several times reported [1, 4, 8], those melts which lead to the amorphous state by rapid quenching show a shoulder at the second peak of the structure factor or of the pair correlation function. In the present case of molten $Cu_{84.3}P_{15.7}$, the second peak of the structure factor is symmetric whereas the second peak of the pair correlation function shows a shoulder.

In Fig. 1 the total structure factors of molten and amorphous $Cu_{84.3}P_{15.7}$ are compared. Both curves show a pronounced secondary peak, which lies for the amorphous state at 1.36 Å^{-1} with a width of 0.65 Å^{-1} and is clearly larger than for the melt (0.52 Å^{-1}). The main peak lies at 3.07 Å^{-1} and is about 65% higher than that of the melt. It is also narrower (0.42 Å^{-1}) than that of the melt (0.56 Å^{-1}), which indicates a stronger localisation of the atoms in the solid state. The stronger attenuation of the melt curve is caused by the thermal motion. The second maximum of the structure factor as obtained from amorphous $Cu_{84.3}P_{15.7}$ is clearly splitted into two maxima at 5.29 Å^{-1} and 5.79 Å^{-1} (heights 1.47 and 1.26). The third maximum lies at 7.74 Å^{-1} (width: 0.84 Å^{-1}).

In Fig. 2 the pair correlation functions obtained from amorphous and molten $Cu_{84.3}P_{15.7}$ are compared. The amorphous state has 12.3 nearest neighbours at a distance of 2.56 Å. The second peak is split into two maxima at 4.40 Å and 5.00 Å, yielding a weighted average distance of 4.66 Å. This splitting was already indicated in the pair correlation function of

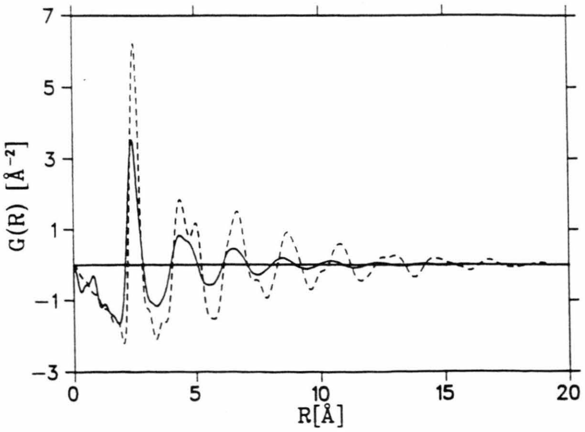

Fig. 2. Total pair correlation functions from $Cu_{84.3}P_{15.7}$; X-rays;
--- amorphous state; ADXD (Mo-K_α),
— molten state (760 °C); EDXD-method.

Table 2. Molten $Cu_{84.3}P_{15.7}$ at 760 °C and amorphous $Cu_{84.3}P_{15.7}$ at room temperature. Pair correlation function. Position R_i, full width at half maximum ΔR_i, and coordination number Z_i.

		$Cu_{84.3}P_{15.7}$ melt	$Cu_{84.3}P_{15.7}$ amorphous
First peak	R_1 [Å]	2.46	2.56
	ΔR_1 [Å]	0.46	0.42
	Z_1	12.1	12.3
Second peak	R_2^A [Å]	4.37	4.40
	R_2^B [Å]	–	5.00
	ΔR_2 [Å]	0.94	1.12
	Z_2	49.2	44.9
Third peak	R_3 [Å]	6.48	6.65
	ΔR_3	0.91	0.80

the molten state by a weak shoulder. The third coordination sphere lies at 6.65 Å (width 0.8 Å).

We state that the radii of all coordination spheres are smaller for the melt than for the amorphous state. Evidently a large free volume is built in the amorphous alloy during the sputtering process. The peak positions R_i, full widths at half maximum ΔR_i, and coordination numbers Z_i of amorphous and molten $Cu_{84.3}P_{15.7}$ are compiled in Table 2.

3.3 *Short range order in amorphous and molten $Cu_{84.3}P_{15.7}$*

The total Bhatia-Thornton structure factor $S^{BT}(Q)$ is composed of three partial structure factors, where S_{NN} stands for the density-density correlations, S_{CC} for the concentration-concentration correlations, and S_{NC} for the contribution caused by the difference of the atomic volumes of both species. In the case of X-ray diffraction with $Cu_{84.3}P_{15.7}$ one has

$$S^{BT}(Q) = 0.965 \cdot S_{NN}(Q) + 0.035 \cdot S_{CC}(Q) + 1.008 \cdot S_{NC}(Q). \quad (1)$$

Non-crystalline materials show very often a prepeak at a Q-value Q_p on the low Q-side of the first peak which lies at Q_f, where $0.5\,Q_f \le Q_p \le 0.7\,Q_f$.

Such a prepeak is a measure for the degree of chemical short range order within the corresponding alloy and belongs to $S_{CC}(Q)$. Now, in the present case the "secondary peak" lies at $Q_p/Q_f = 0.44$ for the amorphous, and at 0.46 for the molten alloy and therefore slightly outside the usual region for a prepeak. Also the weighting factor for $S_{CC}(Q)$ in (1) is so small that a real prepeak in this case could not be observed. In [9] it was shown that also for neutron diffraction using the method of isotopic substitution there is no chance to evaluate $S_{CC}(Q)$. Thus, for the $Cu_{84.3}P_{15.7}$-alloys a real prepeak cannot be deteced, neither with X-rays nor with neutrons, and it is suggested that the secondary peak as observed in Fig. 1 belongs to $S_{NN}(Q)$ or $S_{NC}(Q)$.

3.4 *Small angle scattering with amorphous $Cu_{84.3}P_{15.7}$*

The fundamentals of small angle scattering are described for example in [10]. Small angle scattering experiments with amorphous $Cu_{84.3}P_{15.7}$ were done using Cu-Kα radiation within a Kratky-camera as described in [11] in the region $8 \cdot 10^{-3}\,Å^{-1} \le Q \le 3.6 \cdot 10^{-1}\,Å^{-1}$. The experimental intensity curve was normalized to absolute units using a calibrated Lupolen standard [12]. The measured intensity was desmeared [13] and is shown in Figure 3. From Fig. 3 we learn that amorphous $Cu_{84.3}P_{15.7}$ shows a very strong small angle scattering signal which means that the specimen is rather inhomogeneous. The three regions I, II, and III in Fig. 3 may be characterized as follows:

I) In this region the log-log-presentation gives a straight line with a gradient −3.6, which could be caused by fractal items.

II) In this region the curve is nonlinear, which indicates the presence of further inhomogeneities. To evaluate the deviation we subtract the linear run from the experimental one and obtain the curve

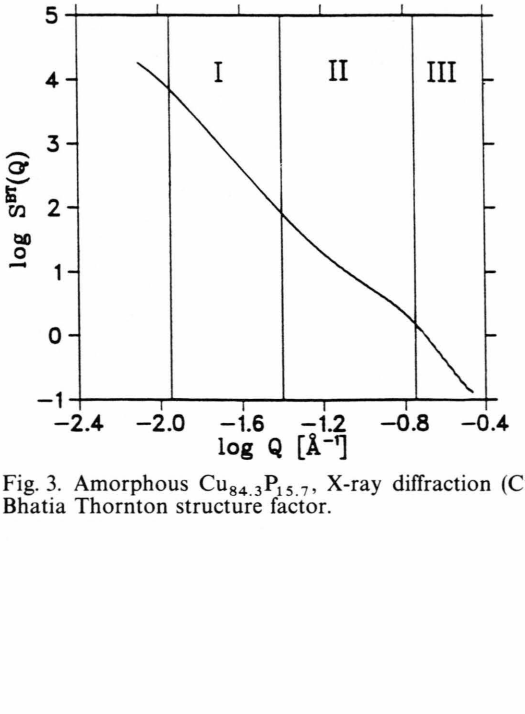

Fig. 3. Amorphous $Cu_{84.3}P_{15.7}$, X-ray diffraction (Cu-K_α). Bhatia Thornton structure factor.

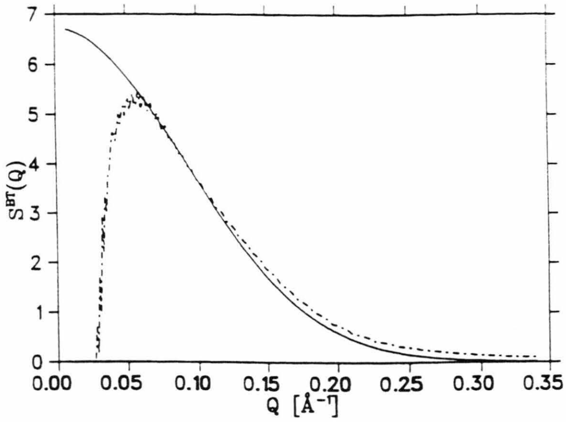

Fig. 4. Amorphous $Cu_{84.3}P_{15.7}$ (–·–·) structure factor. Difference curve. (——) Gauss-fit.

shown in Fig. 4 (broken line). Now we apply Guinier's approach [14] according to

$$I_g(Q) = I(0)\exp\left(-\frac{Q^2 R_g^2}{3}\right). \tag{2}$$

and obtain the full line.

The so called Guinier-Radius R_g is thus found to be 14 Å and corresponds according to the equation

$$R_{\text{ball}} = R_g \cdot \sqrt{5/3} \tag{3}$$

to ball shaped inhomogeneities with radius $R_{\text{ball}} = 18.1$ Å.

III) This region shows a gradient of -4 which was predicted by Porod [15] for inhomogeneities with smooth surfaces.

To decide whether the strong small angle scattering effect is caused by concentration or by density-fluctuations we refer again to (1) and find that according to the weighting factors in the present case probably the density fluctuations predominate.

4. Summary

The structure factor and the pair correlation function of the molten alloy show flat-topped and broadened maxima compared to those of the amorphous alloy. This is caused by the thermal motions in the molten state. The atomic distances in the molten state are smaller than those in the amorphous state which can be understood by free volume which is brought into the amorphous state during its production. Because of the unsuitable weighting factors with which the partial structure factors are multiplied to yield the total structure factor, no conclusions concerning the chemical short range order in amorphous and molten $Cu_{84.3}P_{15.7}$ are possible. The so called secondary peak at about 1.40 Å^{-1} therefore is not a premaximum in the usual sense, from which one could derive the degree of chemical short range order.

Small angle X-ray diffraction with the amorphous specimen showed that this specimen contains regions with a radius of gyration of about 14 Å whose density is definitely different from that of the surrounding matrix.

[1] E. Nold, G. Rainer-Harbach, P. Lamparter, and S. Steeb, Z. Naturforsch. **38a,** 325 (1983).

[2] M. Nuding, Diploma thesis. University of Stuttgart, 1990.

[3] M. Ellner, M. El-Boragy, and B. Predel, in: S. Steeb and H. Warlimont (ed.), Proc. 5th Int. Conf. on Rapidly Quenched Metals RQV, Würzburg 1985, page 183.

[4] E. Nassif, P. Lamparter, B. Sedelmeyer, and S. Steeb, Z. Naturforsch. **38a,** 1093 (1983).

[5] E. Nassif, P. Lamparter, B. Sedelmeyer, and S. Steeb, Z. Naturforsch. **38a,** 1098 (1983).

[6] R. M. Hagenmayer, P. Lamparter, and S. Steeb, Z. Naturforsch. **50a** (1995).

[7] M. Heckele, Diploma thesis, University of Stuttgart, 1988.

[8] B. Sedelmeyer, Doctor thesis, University of Stuttgart, 1985.

[9] R. M. Hagenmayer, Doctor thesis, University of Stuttgart, 1992.

[10] O. Kratky, G. Porod, and L. Kahovec, Z. Elektrochem. **55,** 53 (1951).

[11] M. Schaal, Diploma thesis, University of Stuttgart, 1985.

[12] R. W. Hendricks, J. Appl. Cryst. **5,** 315 (1972).

[13] P. W. Schmidt and R. Height Jr., Acta Cryst, **13,** 480 (1960).

[14] H. Guinier and G. Fournet, Small Angle Scattering of X-rays, John Wiley & Sons Inc., London 1955.

[15] G. Porod, Kolloid-Z. **124,** 83 (1951).